DISTRIBUTED RENEWABLE ENERGY TECHNOLOGIES: DESIGN AND DEVELOPMENT OF SCALABLE TRANSMISSION SYSTEMS

by

Shruti Mohandas Menon

A thesis submitted to the faculty of
The University of North Carolina at Charlotte
in partial fulfillment of the requirements
for the degree of Master of Science in
Mechanical Engineering

Charlotte

2018

Approved by:

____
Dr. Navid Goudarzi

____
Dr. Friedrich Goch

____
Dr. Alireza Tabarraei

____
Dr. Stuart Smith

ABSTRACT

SHRUTI MOHANDAS MENON.
DISTRIBUTED RENEWABLE ENERGY TECHNOLOGIES: DESIGN AND DEVELOPMENT OF SCALABLE TRANSMISSION SYSTEMS. (UNDER THE DIRECTION OF DR. NAVID GOUDARZI)

Renewable forms of energy are being intensively pursued and investigated in systems connected to the grid as well as in standalone applications. The global energy generation is expected to grow 2.7 times by the year 2035. Today, renewable energy resources account for 14% of the total world energy demand. There are however, certain disadvantages associated with the use of alternative energy resources such as intermittency in energy resource, instability, and high initial investment. To meet the growing energy demand, solutions are being explored to overcome the drawbacks associated with the use of these forms of energy.

The goal of this MS thesis is to develop a transmission system, with a focus on the gearbox, for low input speed applications. This system is designed for use in non-traditional renewable energy harnessing technologies such as wind and hydrokinetic energy generation. The goal is pursued through several objectives:

- Conducting theoretical analysis to determine either the required torque or gearbox specifications based on the input torque or desired output torque at defined input speeds.
- Conducting Finite Element Analysis (FEA) on the developed gearbox system to examine the structural stability, using the stress and displacement criteria.

- Developing a prototype for experimental testing.
- Validating the results based on material properties and literature.

The Finite Element Analysis takes into consideration different mesh and geometry environments to predict the accuracy of the results. These predictions, however, are based on a number of assumptions such as perfectly elastic material behavior, disregarding losses due to friction and gear pair misalignments. The findings obtained from the stress distributions in each of the environments are compared with Hertzian contact stress analysis. It is observed that the contact stress (Von Mises) obtained through FEA approach the analytic stress (Hertz) values by determining the optimum mesh density. This is achieved by identifying and refining the mesh in the regions of localized stresses. In case of gear pairs, the maximum stress is concentrated at the contact region of the mating gear teeth. Thus, the gear faces in contact have a refined mesh with a face element size of 0.1 mm. Regions with comparatively lower stress values can be coarse (in this case the maximum element size is 10 mm). Using a "proximity and curvature" or "curvature" type of mesh ensures finer quad meshing in the stress concentrated areas.

One case study for the proposed epicyclic gear design can be found in a distributed wind energy technology system, called Wind Tower Technology (WTT) to be used in Maryland, US. Epicyclic gears are known to have advantages over parallel shaft drives in terms of weight, number of components, and size. These make it a suitable choice for the WTT and similar concepts where a significant increase in the output shaft power is needed. In this case, the gear train configuration is designed based on the output torque requirement, taking into consideration, the materials and ease of machining and manufacturing. Manufacturing techniques such as laser cutting, CNC machining, 3D printing and silicone molding are used to fabricate a two-stage gearbox system and the set up. As a future scope, this setup will be connected to a Data Acquisition System – "LabVIEW" to test the feasibility of the gearbox design by determining the current-voltage characteristics of the generator connected to this system. The FEA results on the final design using Delrin as a material for gears showed a maximum gear tooth contact stress of 37 MPa (the allowable stress defined by ASTM D4181 is 98 MPa) and using steel for shafts showed a maximum stress of 206 MPa (the allowable stress defined by AISI 1020 is 350 MPa).

The second part of this MS thesis is focused on conducting FEA on a speed converter to be used for renewable energy technologies. While current systems control the output power fluctuations electronically, the patented speed converter employ mechanical controls to obtain a smooth output power. Its application for the proposed case is studied and discussed when used in conjunction with the developed epicyclic gearbox system. The results show the potential of obtaining a smooth high-rated power using a combination of proposed epicyclic gearbox system and the speed converter. Further experimental research at different scales can be pursued as a follow up of this research.

ACKNOWLEDGEMENTS

I would like to express my sincere gratitude to my research advisor Dr. Navid Goudarzi for his continuous support, patience and motivation during my Masters thesis study and research. His guidance has helped me in all times in course of my research and writing of this thesis.

Besides my advisor, I would like to thank the rest of my thesis committee: Dr. Stuart Smith, Dr. Alireza Tabarraei, and Dr. Friedrich Goch for their encouragement and insightful comments. I would also like to extend a special thank you to Dr. Wesley Williams for all his help, insight, and encouragement in the fabrication process.

I would like to thank David Barnett and Casey Nichols for their time and help in the prototyping of the system, Anay Joshi for his inputs in FEA, my close friends Shikha Patel, Manali Ghosh, Disha Shirgurkar, Surabhi Deshmukh, Akul Swami, Ila Ragade, Shahrukh Shaikh, Akash Ojha, Abhishek Kshirsagar and Parag Mehare for their moral support throughout my course duration as a Masters student.

Last but not the least, I would like to thank my family: my parents Mr. Mohandas Menon, Mrs. Savitri Menon, and my sister Sheetal for their constant support and encouragement. Without them this would have never been possible.

TABLE OF CONTENTS

LIST OF FIGURES

LIST OF TABLES

NOMENCLATURE

P_d	Diametrical pitch
D	Pitch circle diameter
B	Backlash
m	Module
C	Centre distance
P	Circular pitch
t	Tooth width
h	Tooth depth
H_a	Addendum
D_a	Dedendum
D_t	Tooth depth diameter
D_f	Tooth root diameter
w	Gear ratio
x	Profile shift
P	Power
T	Torque
n	Rotations per minute (rpm)
N	No. of teeth
ϕ	Relative rotational motion
ω	Angular motion

CHAPTER 1: INTRODUCTION

The use of renewable sources of energy, as an alternative to fossil fuels in on a rise in recent years [1]. Wind energy technology has matured to be amongst the lower cost renewable energy systems and has uses in stand-alone applications as well as onshore/offshore generation connected to the grid [2]. In order to overcome the drawbacks associated with wind energy generation, such as its intermittent nature, initial cost of investment and geographical constraints, they are integrated with other forms of energy, both renewable and conventional. Extensive research is also carried out to utilize wind in regions with low velocity or for application in residential or commercial areas. Daryoush Allaei came up with a new concept for non-traditional wind power systems, which significantly outperforms traditional wind turbines of the same structural parameters and aerodynamic characteristics under the same wind loading conditions. It delivers significantly higher output, at reduced cost. The first innovative feature of the design is the elimination of tower-mounted turbines [3]. Venters et.al worked on optimizing a duct design, for ducted wind turbines (DWT). It was observed that for the same rotor area, the power output of the DWT was greater than an open rotor. Experimental analysis carried out found that the increase in power relative to an open rotor depends on the size of the duct i.e. with larger ducts the power progressively increases [4]. Windation Energy Systems Inc. is another company, based of Menlo Park, California, that designs and installs small scale wind energy systems. They actively work towards reducing the turbine size and improving their design methodologies for safe rooftop wind harnessing systems, targeting the urban wind market [5]. Steve Burkle, the inventor of EiP Technologies designed a vertical axis wind machine, for wind energy generation in residential areas [6]. These studies demonstrate that wind catchers and ducts can improve the wind harnessing efficiency and make the use of wind energy possible in regions with low wind speed.

In order to further increase the speed, special attention needs to be paid to the transmission system, the gearbox being a critical component. In the context of distributed wind technologies, there also arises a need for the system to be cost effective along with being efficient. Epicyclic gear sets offer a compact size with higher gear ratios and power densities. Besides applications in wind harnessing technologies, they are also widely used in mechanisms such as industrial drives, automobiles, machine tools, and prime movers [7]. Deciding on the type of gearbox to be used, involves estimating parameters such as speed up ratio, number of stages, gearbox weight and cost, depending on the type of application. In case of a turbine that runs on low velocity wind, the questions that arise in the design phases are operation capability, reliability, maintenance and replacement [8]. Gearbox failures in wind harnessing systems have always been an issue in terms of gearbox reliability. The most common causes of failure include bearing and gear tooth failures (macro-pitting, breakage, and scuffing) [9]. Ragheb et.al in their work have stressed on the failure causes of the gearbox in wind energy applications. Most of these failures have been attributed to the movement of the system setup chassis, causing misalignment of the gearbox with the generator shafts. Regular turbine realignments can reduce the frequency of failure, but do not preclude their occurrence [10]. Nejad et al. studied the factors that lead to gearbox fatigue failures and proposed a long-term fatigue damage analysis for wind turbine drive trains. One of the major causes of gearbox failures are gear tooth root bending. In their study, the authors carried out stress analysis against a range of loads, for fatigue failure analysis using a number of approaches. Another important design parameter that must be considered in failure analysis is material selection. Common gear materials include steel, brass, bronze, cast iron, ductile iron, aluminum, powdered metals, and plastics. Material selection is based on application and is crucial to performance and reliability [11].

Material selection and method of manufacturing are other factors that are an important part of the design process for any system. Plastic is commonly used as a material for prototyping purposes. In this work, the use of Delrin is studied for application in the WTT structure. Duhovnik et al. observed the effects on gear lifetimes and fatigue due to loading at smaller torque values, on plastic gears, through FEA and experimental investigation. Effects on these wear characteristics, based on tooth profile, temperature and method of manufacturing were studied. The material tested was Delrin [12]. Hlebanja et al. identified the solutions for preventing or diminishing micro-pitting occurrences in plastic gears by employing better lubrication, high quality surface treatment (super-finishing), gear tooth flank profile change in the meshing start area, and finally, better materials. They suggested the use of “S” profile gears since they have a more evenly distributed contact point density which implies less sliding and lower power losses [13]. A number of manufacturing processes were explored in this work which includes, laser cutting, CNC, 3D printing and silicone molding, for building the prototype.

CHAPTER 2: DUCTED WIND TOWER TECHNOLOGY (WTT)-CASE STUDY

As a case study, a transmission system is designed for use in a small scale non-traditional wind energy generation system. The ducted WTT structure is designed to utilize low velocity wind speeds in urban settings (residential or commercial), previously constructed and tested on the University of Maryland, Baltimore County site [14].

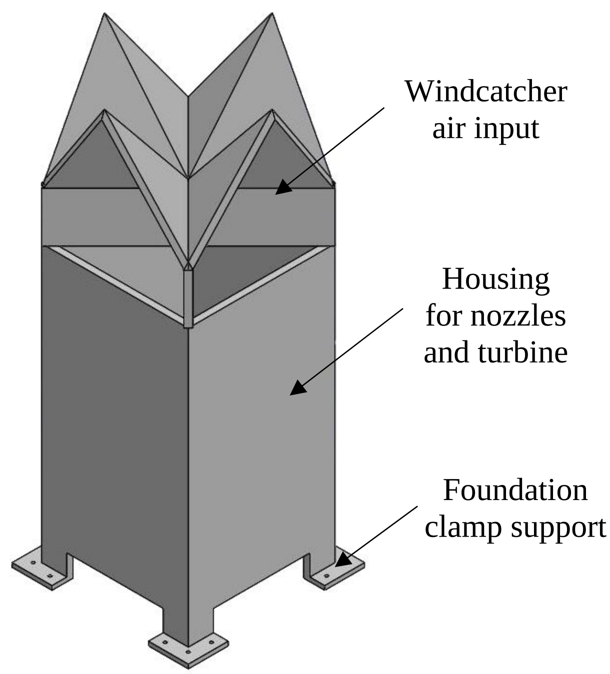

Figure 1: Isometric view of the WTT

It consists of ducts that create a suction effect at the entry and nozzles in the interior to further increase the wind speed. The interior of the tower houses components such as the turbine, gearbox, electricals and cooling system. The studies carried out in the previous works have also demonstrated an increase in the turbine output. In this work, the output power is further increased by the designed gearbox system.

CHAPTER 3: EPICYCLIC GEAR TRAIN DESIGN AND ANALYSIS

An epicyclic gear train, also known as a planetary gear drive, is a more complex drive compared to a parallel shaft spur gear set. These gear sets are mainly used when a large change in speed or power is needed over a small distance and are more compact. In case of the WTT application, the size and weight of the system are important due to space constraints. Also, since there is a need for speed increase, the epicyclic gearbox becomes a suitable choice for this application.

3.1 Gear design procedure:

An epicyclic gear train can operate in multiple configurations. Keeping either the planets, sun or ring fixed, different configurations produce a speed increase or decrease. In the case of the WTT, there is a need for speed increase. Calculating the gear ratios would give the ideal configuration for this application. The following assumptions are made to determine the two-stage epicyclic gear train driver and driven components. Please note that subscripts ‘p’, ‘s’ and ‘r’ denote the planet, sun and ring respectively. As an initial assumption, the diametrical pitch, P_d is 20. Keeping the space constraints in mind and through detailed literature survey, an initial guess on the gear pair dimensions are made to be D_p = 1 inch, D_s = 4.25 inches and D_r = 6.25 inches. To find out the optimum configuration of the epicyclic gear train, speed ratio of four possible combinations is explored and explained in a detailed design methodology [15]. The configuration is the same for both the stages.

Out of the possible configurations, the maximum power increase could have been obtained if the ring is the driving gear and the planets are the driven gears, with the sun being stationary. However, it is observed that there is a difficulty in manufacturing the test setup for this configuration, since it makes it excessively bulky and heavy, adding components to the system. This in turn could lead to undesirable power losses. Thus, the most suitable configuration, keeping increased power output and ease of manufacturing in mind would be the one where the sun is the driving gear, planets are the driven gears and the ring is stationary. Both the stages have the same configuration and the overall gear ratio would be 1:18.

The spur gear design procedure is based on standard available design equations for internal gears. All dimensions calculated are in inches. Based on a literature survey and study of numerous types of gear design procedures, the pressure angle is selected at 20º, for low input speed applications.

1. Backlash for planet and ring gear:

$$B_p = \frac{0.04}{D_p} = \frac{0.04}{1} = 0.04\,\text{in} \tag{1}$$

$$B_r = \frac{0.04}{D_r} = \frac{0.04}{6.25} = 0.0064\,\text{in} \tag{2}$$

2. Gear module:

$$m = \frac{D_p}{N_p} = \frac{D_r}{N_r} = 0.05\,\text{in} \tag{3}$$

3. Gear tooth width:

To find the gear tooth width, the circular pitch needs to be calculated first, which depends on the center distance between the two gears.

$$C = \left(\frac{D_r}{2}\right) - \left(\frac{D_p}{2}\right) = \left(\frac{6.25}{2}\right) - \left(\frac{1}{2}\right) = 2.62\,\text{in} \tag{4}$$

Using the calculated value of center distance

$$P = \frac{2\pi C}{N_r - N_p} = \frac{2\pi \times 2.625}{125 - 20} = 0.15\,\text{in} \tag{5}$$

The above obtained value of circular pitch is used to calculate the tooth width

$$t_p = \frac{1}{2}\left(P_p - B_p\right) = \frac{1}{2}\left(0.157 - 0.04\right) = 0.05\,\text{in} \tag{6}$$

$$t_r = \frac{1}{2}\left(P_p - B_r\right) = \frac{1}{2}\left(0.157 - 0.0064\right) = 0.07\,\text{in} \tag{7}$$

4. Tooth depth:

$$h = 2.25 \times m = 2.25 \times 0.05 = 0.11\,\text{in} \tag{8}$$

5. Addendum and Dedendum:

Addendum and dedendum shift, also known as addendum modification or correction, is the displacement of the rack or cutting tool datum line from the reference diameter of the gear. This is a standard value which is 0.516 in for internal gears and 0 for external gears. The value of profile shift is used to calculate the addendum and dedendum values.

$$H_{ap} = (1 + x_p) \times m = (1 + 0) \times 0.05 = 0.05\,\text{in} \tag{9}$$

$$H_{ar} = (1 + x_r) \times m = (1 - 0.516) \times 0.05 = 0.02\,\text{in} \tag{10}$$

The total depth and addendum are known, thus the dedendum can be calculated as

$$D_{ap} = (h - H_{ap}) = (0.1125 - 0.05) = 0.06\,\text{in} \tag{11}$$

$$D_{ar} = (h - H_{ar}) = (0.1125 - 0.0242) = 0.08\,\text{in} \tag{12}$$

While designing gears, it is important to determine the gear size by considering clearance values. The addition of clearances eliminates backlash errors, reduces noise and vibration.

6. Tip diameters:

$$D_{tp} = D_p + 2 \times H_{ap} = 1 + (2 \times 0.05) = 1.1 \text{ in} \tag{13}$$

$$D_{tr} = D_r - 2 \times H_{ar} = 6.25 - (2 \times 0.024) = 6.20 \text{ in} \tag{14}$$

7. Root diameters:

$$D_{fp} = D_{tp} - 2 \times h = 1.1 - 2 \times 0.112 = 0.87 \text{ in} \tag{15}$$

$$D_{fr} = D_{tr} + 2 \times h = 6.20 + 2 \times 0.112 = 6.42 \text{ in} \tag{16}$$

The final dimensions of the planet ring gear pairs are listed below. The sun gear dimensions can be easily determined with the calculated clearance values when the ring and planet dimensions are known.

Table 1: Final dimensions of the Planet – Ring gear pair

Parameter	Planet (inch)	Ring (inch)
w	0.16	0.16
Φ	20	20
B	0.04	0.0064
C	2.62	2.62
P_p	0.15	0.15
t	0.05	0.07
h	0.11	0.11
H_a	0.05	0.02
D_a	0.06	0.08
D_t	1.10	6.20
D_f	0.87	6.42
x	0	0.51

3.2 Torque calculation:

Based on previous studies carried out on the UMBC site, the average power output of the turbine from the WTT structure is computed [16]. Figure 2 graphically represents the turbine output power Vs the input wind speed. In their work, Goudarzi et al, carried out Computational Fluid Dynamics (CFD) analysis to determine the turbine output speeds at different input wind speeds. These results are used to find out the gearbox torque requirements. A sample calculation is presented for a wind speed of 2 m/s, since for speeds over a range of 2 m/s to 5 m/s, an alternative method to shut the turbine must be considered. This is majorly to avoid overdesign of the system by taking non-recurring weather conditions into consideration.

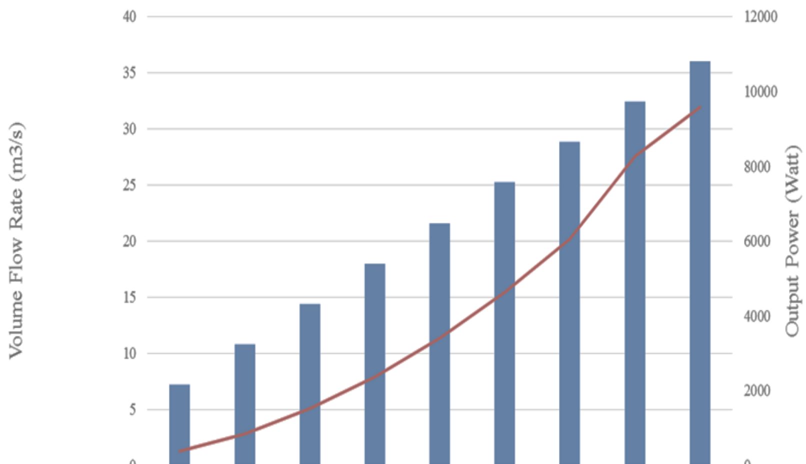

	2	3	4	5	6	7	8	9	10
Volume Flow Rate	7.2	10.8	14.4	18	21.6	25.2	28.8	32.4	36
Output Power	375	850	1525	2365	3400	4625	6050	8275	9575

Figure 2: Turbine output power and volume flow rate at different wind speeds. Reprinted from Goudarzi, N., Zhu, W. D., & Bahari, H. (2014, August). Numerical Simulation of a Fluid Flow Inside a Novel Ducted Wind Turbine. In ASME 2014 4th Joint US-European Fluids Engineering Division Summer Meeting (pp. V01DT39A006-V01DT39A006)

In this work, the minimum and maximum output power of a turbine in the WTT which correspond to the 2 m/s and 10 m/s, respectively, are used to calculate the turbine output shaft torque values for three rotational speeds of 100 rpm, 300 rpm, and 500 rpm. These speed ranges are selected based on motor specifications. The gearbox minimum input torque is calculated from the power equation for the minimum wind speed i.e. 2 m/s. From the turbine power output available to us we can calculate the input torque to the gearbox, assuming no mechanical losses.

$$P = \frac{2\times\pi\times N\times T_{in}}{60} = \frac{2\times\pi\times 100\times T_{in}}{60} = 375\,\mathrm{W} \tag{17}$$

$$T_{in} = 35.80\,\mathrm{N\cdot m}$$

Similarly, the values of T_{in} for the speeds of 300 rpm and 500 rpm are 11.93 N·m and 7.16 N·m, respectively. With the gear ratio the output torque can be determined. The overall gear ratio in this case is 1:18, which will determine the input torque to the hummingbird speed converter.

$$w = \frac{T_{out}}{T_{in}} \tag{18}$$

$$T_{out} = \frac{35.809}{18} = 1.99\,\mathrm{N\cdot m}$$

3.3 Design Algorithm:

A CAD model of the assembly is created in SolidWorks and the entire setup for the assembly, including the base rail fittings, motor and generator mounts are designed. Standard dimensions for shafts and couplers are used. The material selected is Delrin for the gears while steel shafts are used to connect the gearbox stages. In order to make the design highly user centric, the design is linked to a series of MATLAB codes and spreadsheets that can be used as an input platform. Figure 3 shows a flowchart outlining the working of the algorithm. MATLAB codes are written to help select a generator type, based on the output torque values, when the user defines an input in the form of the planet, sun and ring dimensions. This methodology is useful when there arises a space constraint and the maximum achievable output torque needs to be determined. Similarly, if the required output torque values are known, the code can be run to find out the required gear dimensions. These dimensions can then be fed onto a spreadsheet that is linked to the CAD model and be updated. This procedure makes further analysis easy to conduct and provides a more concise approach to account for variability in designs. It may be noted that SolidWorks has an inbuilt feature to create parts of any transmission system known as 'Design Library'. However, there are two limitations to this feature. Design library is not an add-on in all versions of SolidWorks. Also, the number of parameters that need to be input are more than those needed in a linked spreadsheet, since the spreadsheet provides options to decide the dependent and independent variables. This process can be more concise by incorporating macros into the SolidWorks design.

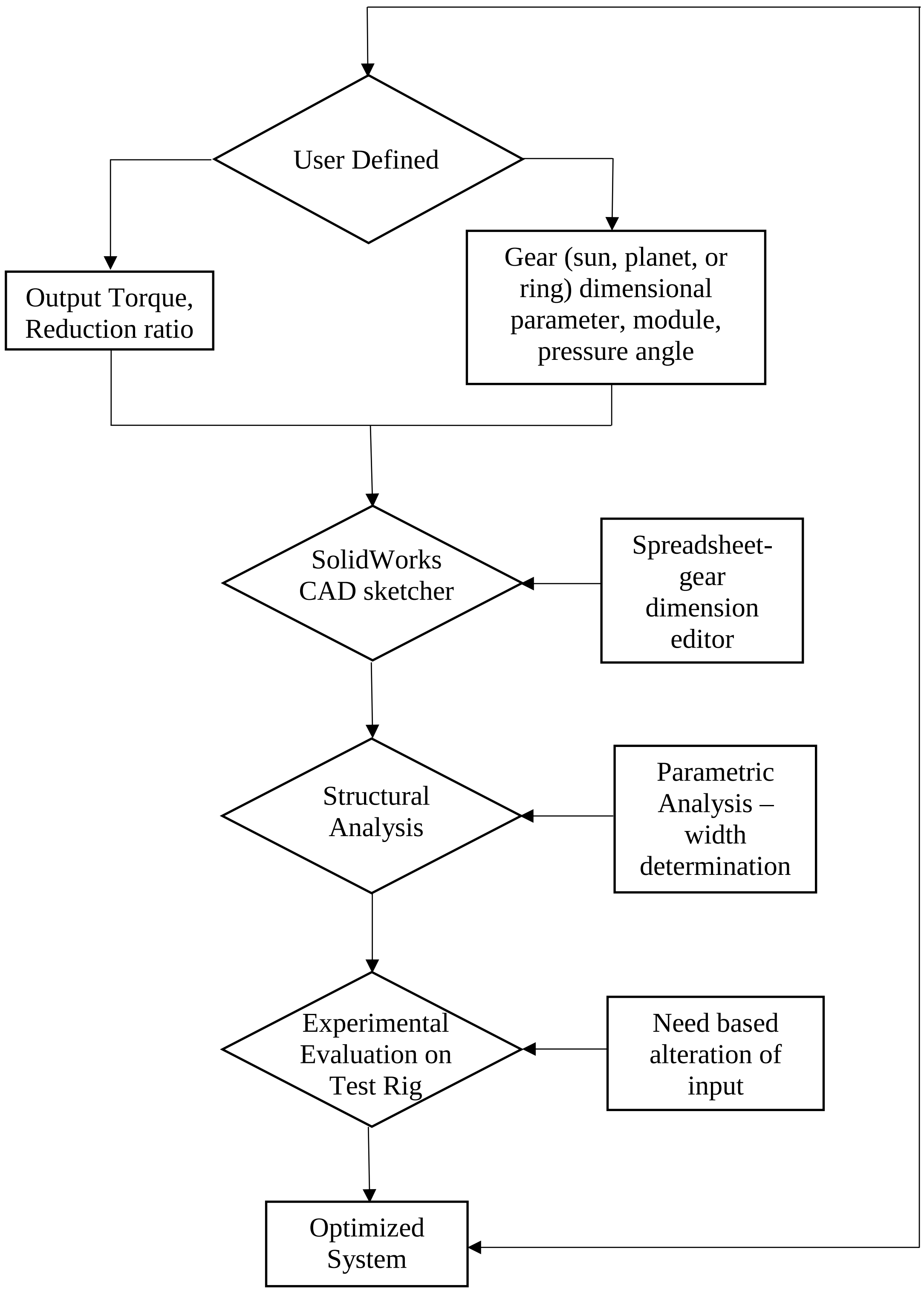

Figure 3: Flowchart outlining the design methodology

3.4 Design conceptualization:

A number of configurations can be selected for the planetary gear sets based on the application need (speed increase or speed decrease). Out of the configurations suitable for this type of gearbox, the initial selected configuration required power input to the ring, which in turn drives the planet, keeping the sun fixed for the first stage. However, it was observed that this configuration would make the system bulkier along with an increase in the number of components that would have to be added to fix the sun. Figure 4 below details the system assembly of the selected configuration which takes ease of manufacturing into consideration. The selected configuration gives 18 times the input shaft speed at the output. To test the functioning of the system under different loading conditions, for the selected material, a test setup is designed. The input is given using a stepper motor (NI-NEMA 34) and the output is obtained through a generator (T-motor U10 KV 100).

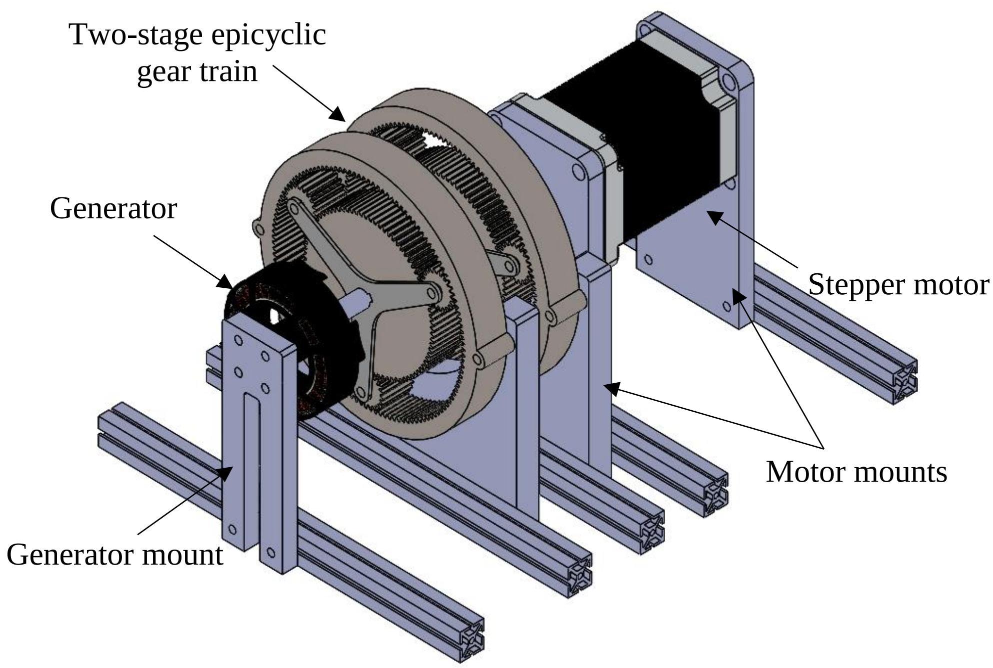

Figure 4: System Design

3.5 Finite element analysis:

Finite element methods are the foundation of mechanical or structural simulations. Finite Element Analysis (FEA) is a computerized method for predicting how a product reacts to real-world forces, vibration, heat, fluid flow, and other physical effects. FEA shows whether a product will break, wear out, or work the way it was designed to. For this system, the analysis is carried out in ANSYS Workbench 14 and 19. The epicyclic gear train is analyzed for structural stability against the turbine output torques.

3.5.1 Methodology:

Static structural analysis is carried out on ANSYS workbench. The gear bores for both the planet and sun gears are set as frictionless supports. A moment/torque (calculated above) is applied on the sun gear bore, since the input shaft is connected to the sun gear. Von Mises stress and total displacement are computed for three cases as discussed below. Finite Element Analysis for any system can be carried out in several environments. For instance, the type of mesh that needs to be selected based on the number of stress concentrated areas, the element type and size, mechanism dependent contact type and solver method. In this work, four environments were explored and validated with the Hertzian contact stress analysis (see appendix B). This study also presents the differences in accuracies in all the four environments.

While analyzing any system, it is important to identify the critical components. For a gearbox, the meshing gears' line of contact, fillets and other existing stress concentration areas depending on the geometry, become critical. A disintegration approach is used for the gearbox analysis where the gearbox is analyzed separately as a meshing pair. This approach helps give a detailed understanding of how the gear teeth react to the applied loads. Based on CFD simulations from previous studies carried out at the UMBC site, the average power output of the turbine for different wind speeds are computed. Considered as an average, the power output corresponding to 2 m/s is used for calculation of the input torque to the turbine. In cases of higher wind velocities that may occur due to bad weather conditions such as hurricanes, the entire system will have to be shut down. Using values of turbine output for wind velocities higher than 2 m/s will lead to an overdesign of the system. The following methods were explored to validate the FEA for the gearbox system to be used as a part of this case study.

Method 1:

The contact faces of the mating gears are given a finer mesh (maximum element size: 0.0001 m), since stresses are higher on the contact point of the mating teeth. The sun and planet gear pair are analyzed with a moment applied to the sun gear. Since gears have multiple stress concentrated regions, the “proximity and curvature” mesh type is used on the mating gear teeth faces, which ensures a refined mesh in the stress concentrated regions.

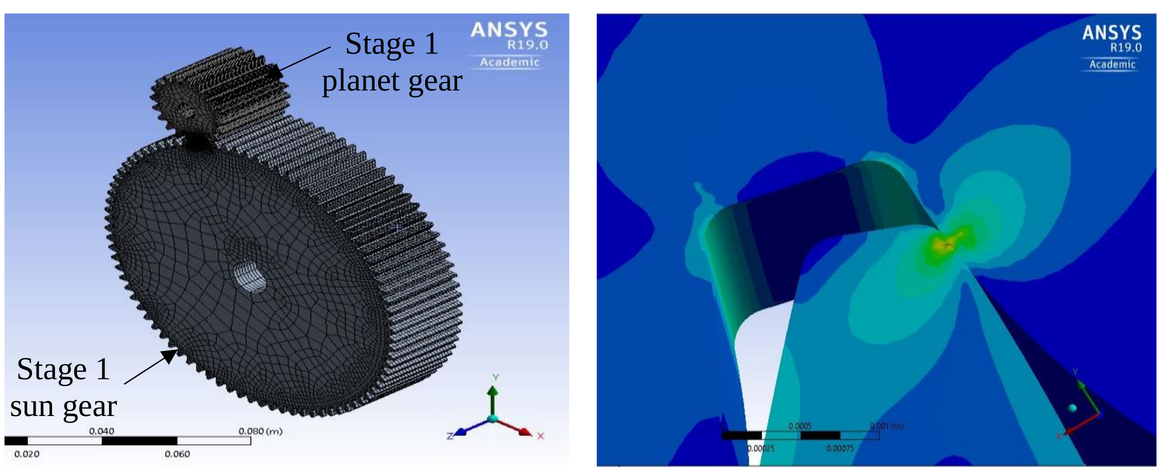

Figure 5: Gear pair analysis in the full-scale model(left) – Von Mises stress at point of contact of the sun-planet gear pair (right)

Method 2:

An optimized analysis technique involves utilizing lesser number of nodes to achieve a prediction of the stresses and displacements. Method 2 presents the use of a scaled model to analyze the stresses. The moment is also proportionally scaled based on the area of gear tooth force application. The mesh environment is set similar to method 1. It is observed that the contact stresses in the scaled model are closer to the values obtained through the Hertz contact stress theory. This is thus achieved with a finer mesh, lesser overall number of nodes and reduced computation time compared to method 1.

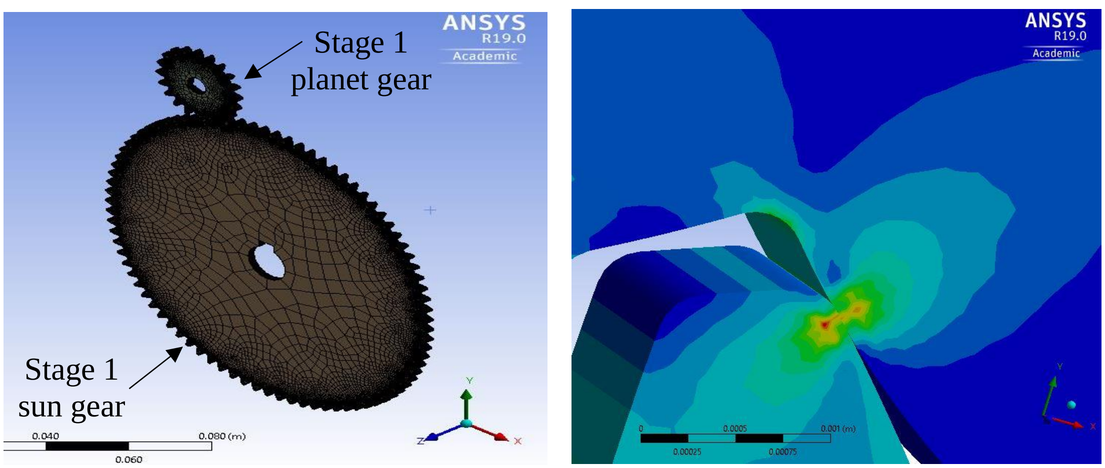

Figure 6: Gear pair analysis on the scaled model (left) – Von Mises stress at point of contact of the sun-planet gear pair (right)

Method 3:

Gear tooth stresses are often calculated by considering the tooth as a cantilever beam. Kawalec et al. presented a comparative analysis of tooth-root strength evaluation methods used within ISO and AGMA standards and verifying them with developed models and simulations using the finite element method [24]. Therefore, finite element analysis (FEA), which can involve complicated tooth geometry, is now a popular and powerful analysis tool to determine tooth deflections and stress distributions. However, applying constraints on a single gear tooth to calculate the contact stresses may lead to artificially high contact stress values in the results, since the stresses are distributed and not concentrated to a single tooth in the process of gear pair meshing. To validate this, a single gear tooth is considered. A fixed constraint is applied on the tooth base and a force is applied on the nodes in the contact region of the mating gear teeth. It must be noted that since contact stresses are developed due to resistance of the driven tooth to the driving tooth motion, one face of the tooth must also be fixed while a load is applied to the nodes of the other. Literature suggests that static analysis must be carried out over at least three gear teeth, since the load distribution at any instant is observed over a minimum of three teeth of the meshing gears as a result of which method 3 simulations observe a higher stress range compared to those in method 1 and 2 [20,21].

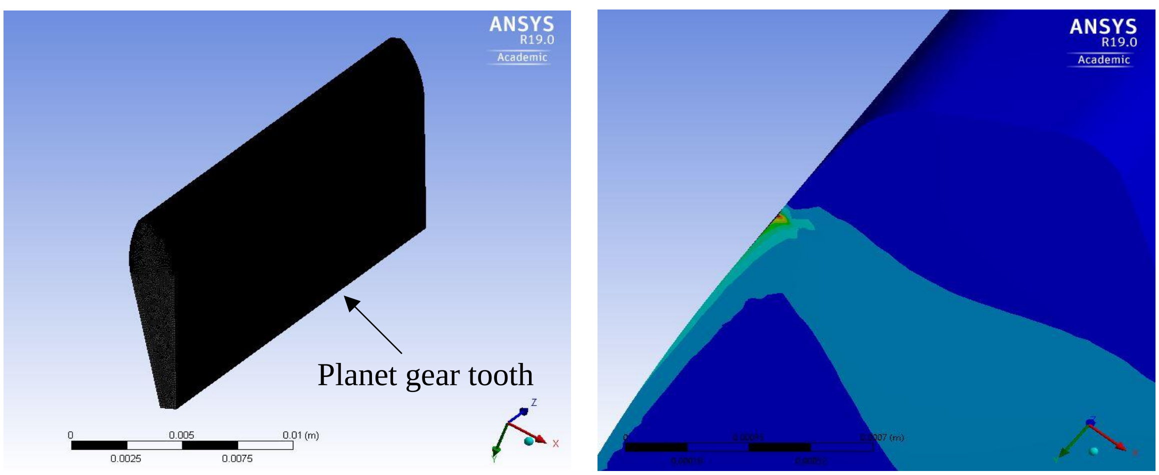

Figure 7: Single gear tooth analysis (left) – Von Mises stress due to sun gear contact on the planet gear tooth (right)

Method 4:

Analysis of individual gear pairs is based on the assumption that there exists equal load distribution between the sun and the planets. The structural analysis of the entire system gives an understanding of how the different connecting parts respond to a single input loading condition. However, it is observed that there is a higher deviation in the observed stress values when the gearbox is analyzed as a whole, compared to analysis of individual gears pairs. The process of obtaining an optimized mesh for larger systems is complex and requires a higher computation time. The findings of this work demonstrate that FEA models for complex systems can be disintegrated and analyzed to obtain results that more closely align with the Hertz contact stress theory. Figure 8 shows the stress distribution pattern for FEA on the gearbox system.

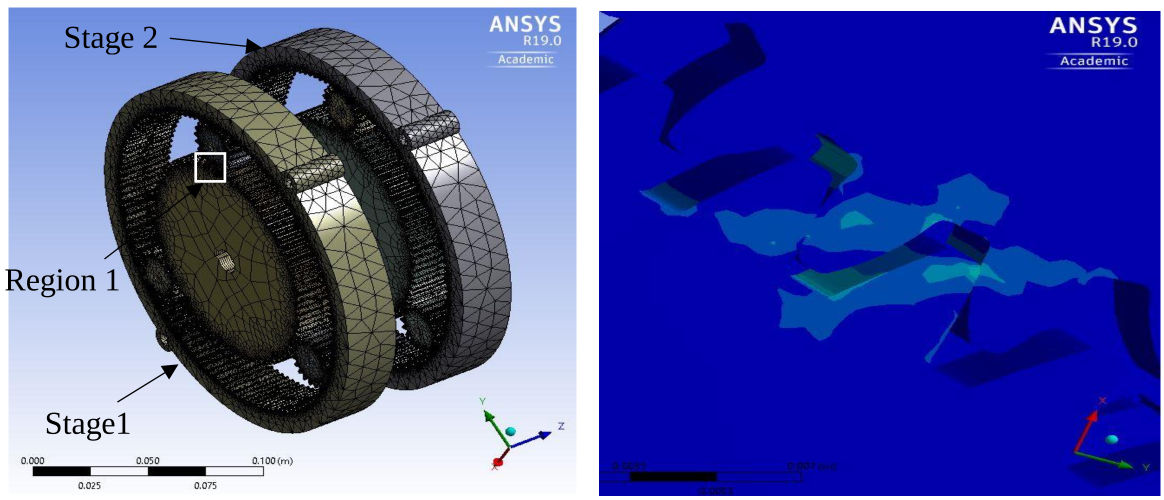

Figure 8: Two-stage epicyclic gearbox (left) – Von Mises stress at point of contact of the sun-planet gear pair stage 1 – Region 1 (right)

3.5.2 Results:

Table 2 below shows the results obtained from FEA. These results are validated by checking for permissible/allowable stress limits that are extracted from material data sheets. Analytical Hertzian contact stress analysis is also carried out to validate these results. Based on the material data sheet (ASTM D4181), the permissible stress for Delrin is 98 MPa. The deviation of the FEA results from the calculated Hertzian contact stresses is also tabulated.

Table 2: Maximum induced stresses corresponding to the analysis type

Analysis type-Static Structural	Contact stress: Von Mises Stress (MPa)	Deviation of FEA from Analytic contact stress values (Percentage)
Hertzian contact stresses	28	
Method 1	31	9.67
Method 2	27	3.5
Method 3	149	81.2
System Analysis	37	24.32

Figure 9 shows a comparison of the results obtained through a parametric analysis carried out on the gear pair, and the Hertz contact stress analysis. The thickness of the planet-sun pair was varied over a range of 2 mm to 4 mm and the corresponding stress distribution patterns were observed. Simultaneously the Hertzian contact stresses were also varied with the thickness.

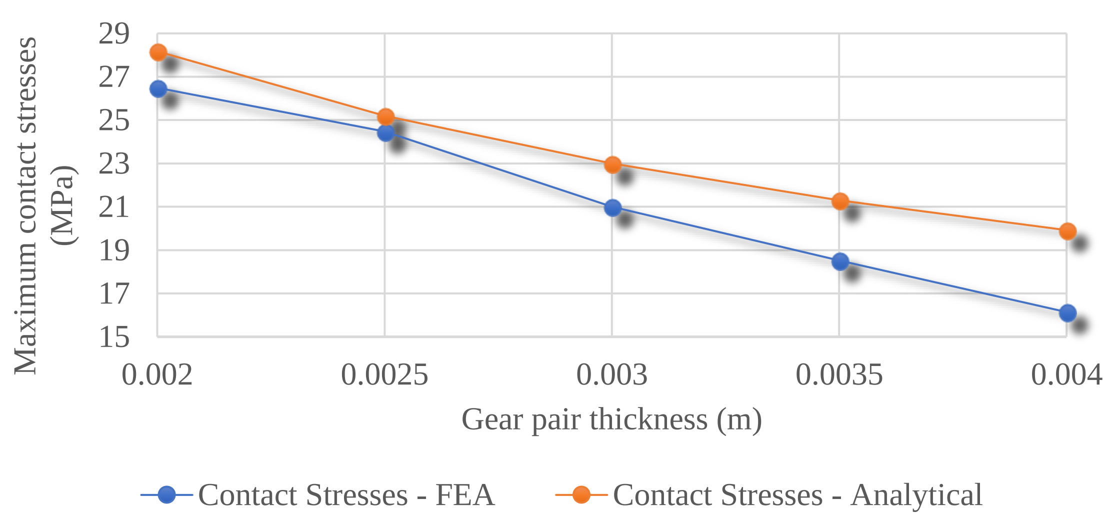

Figure 9: Comparison between contact stresses- Analytical and FEA

3.5.3 Prototype:

Figure 10 and 11 below shows the manufactured gear parts and the mounts. The gears are made of Delrin and are machined using CNC and the mounts made of Acrylic are cut using laser cutting technique. The CNC milling machine, manufactured by Carbide 3D, uses “Carbide Create” (Nomad 883) to generate a G-code. The laser cutting machine on the other hand, uses “Inkscape” to convert the .dxf extension file into pdf, which is then sent as an input to the laser cutting machine. The initial test setup is a scaled prototype with gear dimensions in full scale and thickness in reduced scale (0.25 inch). Figure 10 and 11 show the epicyclic gear stage 1 and the ring support, motor and generator mounts.

As a future scope, this gearbox will be tested to validate its structural stability to the input loading conditions. A stepper motor (NI-ST34-01) is used as input to the gearbox. The output of the gearbox is connected to a generator (T motor, 80 rpm, U10). This setup is connected to a Data Acquisition System (DAQ)-LabVIEW. The output I-V (Current and Voltage) characteristics would be used to test the generator response with the input from the motor. The tests results could be then used to understand the gearbox functioning for the WTT application. By varying the input motor shaft rpm, this system can be tested for use in other similar low input speed applications.

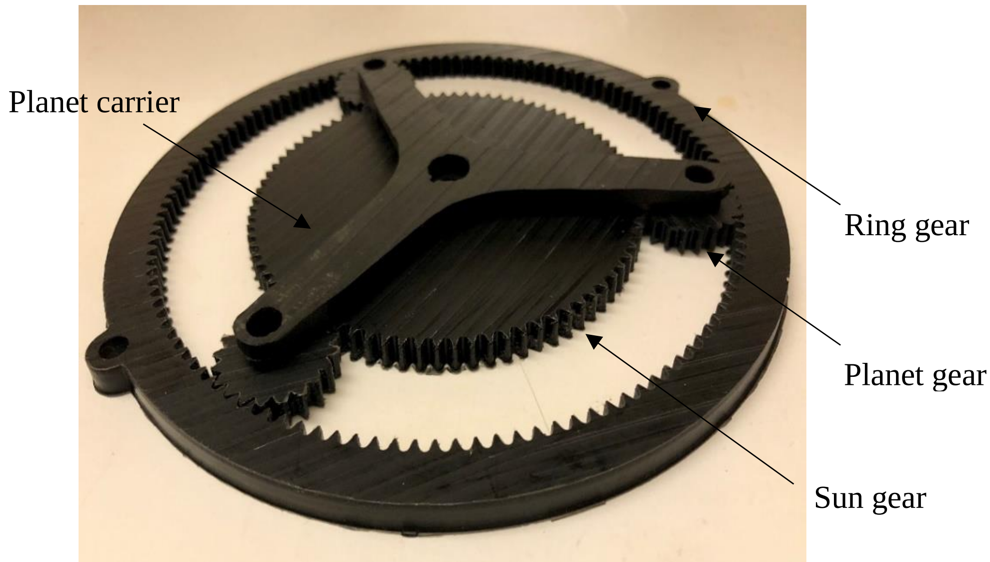

Figure 10: Fabricated gear parts

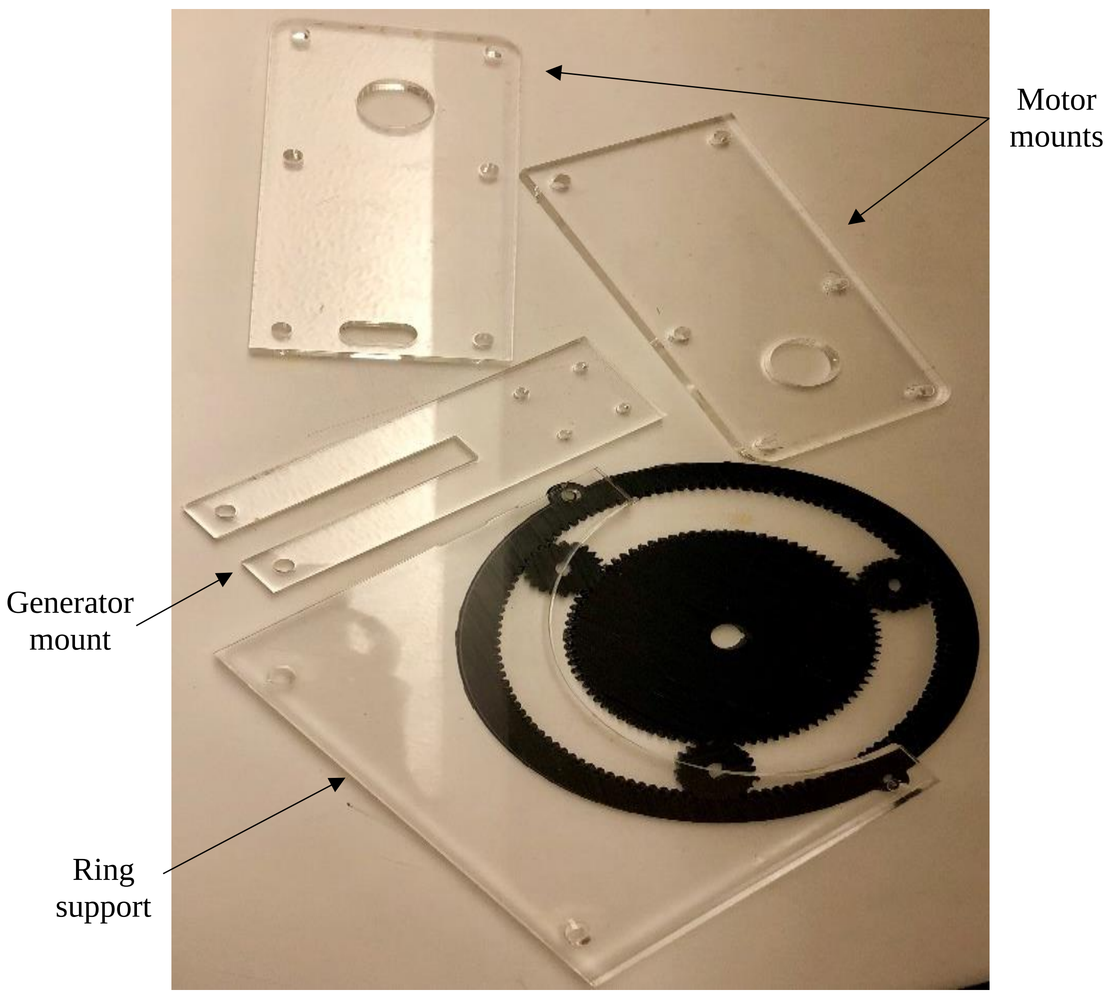

Figure 11: Fabricated ring support, motor and generator mounts

CHAPTER 4: HUMMINGBIRD SPEED CONVERTER

With the growing usage of renewable sources of energy, there is also a need to reduce the drawbacks associated with the use of these resources. One of the drawbacks addressed in this work is variability. Wind speeds vary constantly resulting in a fluctuating output, unsuitable for the electric grid, which makes the use of power electronics imperative. Existing designs solve this problem by using power converters that convert AC to DC power and DC back to AC power. A solution to convert variable output to constant, before power has been generated, was developed by Differential Dynamics Corporation (DD Motion), a Maryland based company [26]. The engineers at DD Motion tested the system for use in hydrokinetic energy generation. In this work, the use of this system, is studied in conjunction with the epicyclic gearbox, for the WTT application. The device introduced in this work is called a Hummingbird speed converter, designed, developed and patented by DD Motion. It is made up to two gear assemblies, called transgears. Figure 12 shows the CAD model of the Hummingbird speed converter. The working of a transgear is similar to that of a differential in an automobile. A detailed analysis of the working of the hummingbird speed converter, how it converts variable speed to constant speed output, structural analysis, and results is presented in this work. The parts of the converter are analyzed using the torque values of the gearbox output. Static structural analysis is carried out in ANSYS Workbench-19 to understand the structural stability of the system to withstand the maximum gearbox output torque, material being stainless steel. The first and second stage sun and meshing planets are analyzed in the order of meshing. While it can be argued that using an additional mechanical system in the transmission of the WTT turbine would lead to additional power losses, experimental studies carried out in previous works show a relatively good power output.

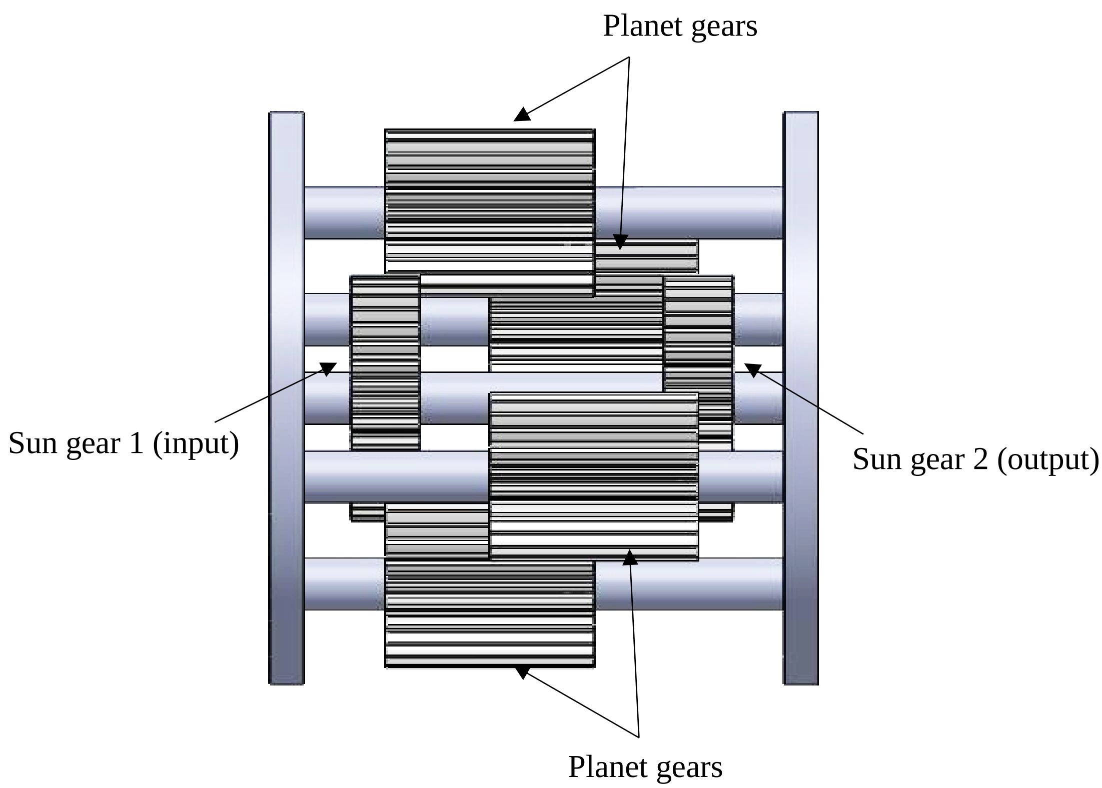

Figure 12: Transgear CAD model

4.1 Methodology:

The input is given to the first stage sun and second stage sun gives the output. Thus, the gear ratio is -1, if the carriers are considered fixed. The relationship between the sun and carrier speeds can be found using the following analysis:

Let the control speed on s_1 be -x.

$$w = \frac{n_{s_1}}{n_{s_2}} \tag{19}$$

But,
$$\frac{n_{s_1}}{n_{s_2}} = -\frac{N_{s_2}}{N_{s_1}} \tag{20}$$

Now, if the carrier is allowed to move,

$$\begin{aligned} \phi_{s_1} &= n_{s_1} - n_c \\ \phi_{s_2} &= n_{s_2} - n_c \end{aligned} \tag{21}$$

Also, the gear ratio follows the equation,

$$r = \frac{\phi_{s_1}}{\phi_{s_2}} = \frac{n_{s_1} - n_c}{n_{s_2} - n_c} \tag{22}$$

Differentiation the angular motion gives the angular velocity

$$\omega_{s_1} - \omega_c - r(\omega_{s_2} - \omega_c) = 0 \tag{23}$$

We know the value of r is -1. Substituting this in the equation above we get

$$\omega_c = \frac{\omega_{s_1} + \omega_{s_2}}{2} \tag{24}$$

Thus, the carrier speed is the average of the speed of the sun gears. Let the input speed be -X. In that case the output speed would be X + ΔX. The carrier speed as per equation no. 24 is (-X+X+ΔX)/2, which is ΔX/2. To obtain the same output as the input, a hummingbird design as shown below is developed. Therefore, with an input of -X rpm the output is -X rpm.

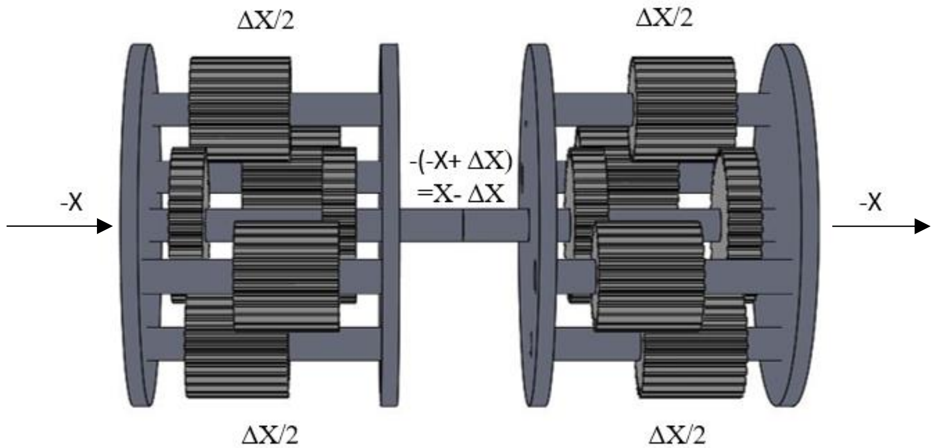

Figure 13: Hummingbird Speed Converter

4.2 Finite Element Analysis – Structural

As mentioned, the hummingbird speed converter is designed for use in hydrokinetic energy. In this work, the focus is on exploring its use in other form of renewable energies, especially wind energy. Based on the output of the designed gearbox, structural analysis is carried out on the hummingbird speed converter to understand how the system reacts to the applied loads. The material used is stainless steel. However, with further research, different materials that help reduce the weight as well as the cost, can be considered.

From equation 18 we have the input torque to the Hummingbird converter. Based on the gear ratio, similar to the earlier analysis, the output torque of the different gears at various stages can be calculated. The obtained values are then set as input variables in ANSYS Workbench for structural analysis. Figure 14 outlines the stress distribution for the hummingbird converter. The maximum stress value is 6.26 MPa and is observed in the gear teeth contact region. This falls below the permissible limit of 505 MPa, based on the ultimate tensile strength for steel. It must be noted that further extensive study in mesh generation would be required to evaluate the error between predictions from this model and stresses existing in a real gearbox of this design. As described earlier, a disintegration approach could yield contact stress values close to the Hertzian stress theory, but structural analysis of the hummingbird system as a complete mechanism (like in this case) would require detailed mesh sensitivity analysis.

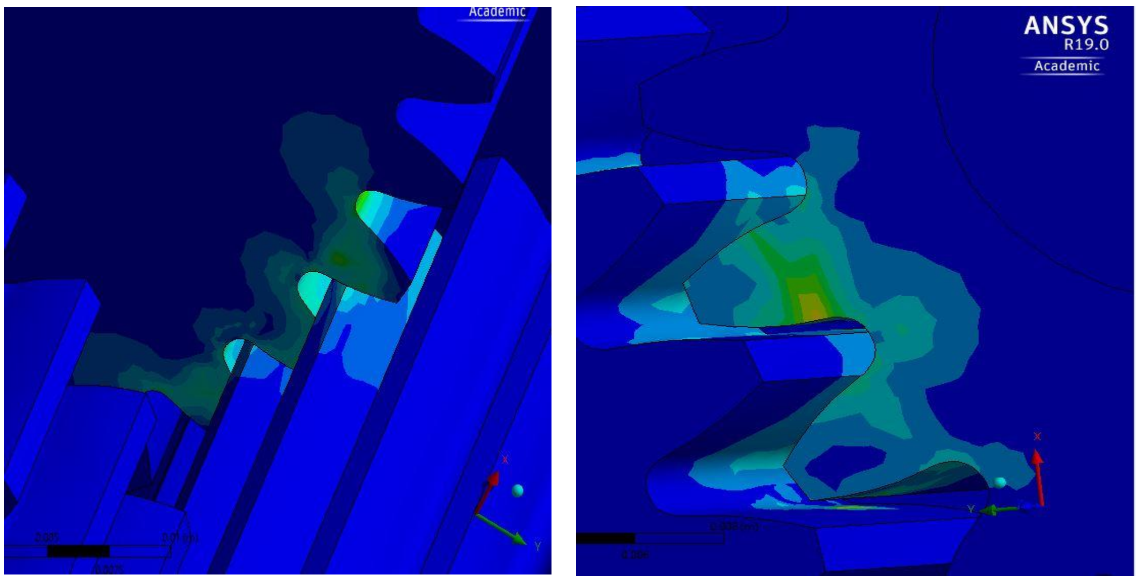

Figure 14: Hummingbird input sun planet gear tooth Von Mises stress distribution (left) - Hummingbird output sun planet gear tooth Von Mises stress distribution (right)

RESULTS, DISCUSSIONS AND FUTURE SCOPE

The objective of this thesis is to obtain maximum output speed in cases of low input speed or high input torque. As a case study, the ducted wind tower is used as an application to design a low input speed scalable gearbox. This work outlines the preliminary results of the design approach. A design methodology is outlined using MATLAB programming to make the system more user centered. This design is validated using Finite Element Analysis and Hertz contact stress theory. The gearbox material is Delrin, which, based on the results from the FEA models, have maximum contact stress values under the permissible material stress limit. Thus, Delrin is considered a suitable choice for a gearbox in this application. Von Mises stresses using FEA is explored using four different methods using the turbine output as the gearbox input

- Full-scale model – The maximum contact stresses observed on the gear teeth is 31 MPa.
- Scaled model – Here the dimensions are in full scale with the thickness scaled to 2 mm and, the moment applied is proportionally scaled based on the area of load application. The maximum contact stresses observed is 27 MPa.
- Single gear tooth – This is based on simple beam theory where a single gear tooth is treated as a cantilever beam with one end fixed and load applied on the other. The maximum contact stress observed is 149 MPa. These high stress values are due to the assumption that the input load acts only on a

single tooth and does not take the load distribution simultaneously acting on the other mating gear teeth.

- The two-stage gearbox system – This method gives an understanding as to how the connected components such the planet carrier and the fixed ring, along with the mating gears, behave to the input loading conditions. Maximum contact stresses on the sun – planet gear pair observed is 37 MPa. It is also observed that FEA conducted by disintegrating this complex system, yields results that approach the analytically calculated contact stresses using the Hertzian contact theory. However, further research must be conducted for mesh analysis when the gearbox is analyzed as a whole to obtain results that more closely agree with the disintegrated model.

The gearbox system and test setup are manufactured and will be tested to validate the results obtained from FEA. In addition to this, a mechanical controller known as the Hummingbird speed converter is analyzed structurally when used in conjunction with the designed epicyclic gearbox. Initially designed and developed for use in hydrokinetic energy in previous works, this patented technology is analyzed for use in the WTT application.

Future Scope:

To validate the results obtained through theoretical Hertz contact theory and FEA, experimental testing is to be carried out. A gearbox is manufactured using CNC with Delrin and the ring support, motor and generator mounts are made of Acrylic using laser cutting technique. For testing, this assembly would be connected to a stepper motor (input) and a generator (output). A DAQ system can be used to study the generator output characteristics to understand the response of the system to the input loading conditions. Currently designed for the WTT application, with changes in the input loading conditions, this system can also be tested for other similar non-traditional renewable energy technologies.

In this work, preliminary steps have been taken to create a test facility. The fabricated gearbox can be tested to validate the current design and findings obtained through the FEA models. These designs can then be improvised and remodeled to reduce the uncertainties in predicted values.

REFERENCES

[1] Dresselhaus, M. S., & Thomas, I. L. (2001). Alternative energy technologies. Nature, 414(6861), 332.

[2] Kaldellis, J. K., & Zafirakis, D. (2011). The wind energy (r) evolution: A short review of a long history. Renewable Energy, 36(7), 1887-1901.

[3] Allaei, D., & Andreopoulos, Y. (2014). INVELOX: Description of a new concept in wind power and its performance evaluation. Energy, 69, 336-344.

[4] Venters, R., Helenbrook, B. T., & Visser, K. D. (2018). Ducted Wind Turbine Optimization. Journal of Solar Energy Engineering, 140(1), 011005.

[5] Calhoon, S. W. (2008). U.S. Patent No. 7,368,828. Washington, DC: U.S. Patent and Trademark Office.

[6] Burkle, S. (2017). U.S. Patent No. 9,803,623. Washington, DC: U.S. Patent and Trademark Office.

[7] Abousleiman, V., & Velex, P. (2006). A hybrid 3D finite element/lumped parameter model for quasi-static and dynamic analyses of planetary/epicyclic gear sets. Mechanism and Machine Theory, 41(6), 725-748.

[8] Jha, A. R. (2010). Wind turbine technology. CRC press.

[9] Musial, W., Butterfield, S., & McNiff, B. (2007). Improving wind turbine gearbox reliability: preprint (No. NREL/CP-500-41548). National Renewable Energy Lab. (NREL), Golden, CO (United States).

[10] Ragheb, A., & Ragheb, M. (2010, March). Wind turbine gearbox technologies. In Nuclear & Renewable Energy Conference (INREC), 2010 1st International (pp. 1-8). IEEE.

[11] Nejad, A. R., Gao, Z., & Moan, T. (2014). On long-term fatigue damage and reliability analysis of gears under wind loads in offshore wind turbine drivetrains. International Journal of Fatigue, 61, 116-128.

[12] TAVČAR, J., GRKMAN, G., & DUHOVNIK, J. (2018). Accelerated lifetime testing of reinforced polymer gears. Journal of Advanced Mechanical Design, Systems, and Manufacturing, 12(1), JAMDSM0006-JAMDSM0006.

[13] Hlebanja, G., Kulovec, S., Hlebanja, J., & Duhovnik, J. (2014). S-gears made of polymers. Ventil, 20(5), 358-367.

[14] Menon, S. M., & Goudarzi, N. (2017, June). Structural Analysis of a Novel Ducted Wind Turbine. In ASME 2017 Power Conference Joint With ICOPE-17 and the ASME 2017 Nuclear Forum (pp. V002T12A003-V002T12A003).

[15] Menon, S. M., & Goudarzi, N. (2017, November). Distributed Wind Energy Technologies: High Speed Scalable Epicyclic Gear Train Design. In ASME 2017 International Mechanical Engineering Congress and Exposition (pp. V006T08A017-V006T08A017). American Society of Mechanical Engineers.

[16] Goudarzi, N., Zhu, W. D., & Bahari, H. (2014, August). Numerical Simulation of a Fluid Flow Inside a Novel Ducted Wind Turbine. In ASME 2014 4th Joint US-European Fluids Engineering Division Summer Meeting (pp. V01DT39A006-V01DT39A006)

[17] Colbourne, J. R. (1990). Geometric Design of Internal Gear Pairs. Gear Technol., 7(3),

28-37.

[18] Nutakor, C., Kłodowski, A., Sopanen, J., Mikkola, A., & Pedrero, J. I. (2017). Planetary gear sets power loss modeling: Application to wind turbines. Tribology International, 105, 42-54.

[19] Kwon, H. S., Kahraman, A., Lee, H. K., & Suh, H. S. (2014). An automated design search for single and double-planet planetary gear sets. Journal of Mechanical Design, 136(6), 061004.

[20] Temis, Yury & Kozharinov, Egor & Kalinin, Dmitry. (2015). Simulation of Gear Systems with Dynamic Analysis. 10.6567/IFToMM.14TH.WC.OS6.029.

[21] Seok-Chul Hwang, Jin-Hwan Lee, Dong-Hyung Lee, Seung-Ho Han, Kwon-Hee Lee, Contact stress analysis for a pair of mating gears, Mathematical and Computer Modelling, Volume 57, Issues 1–2, 2013.

[22] Cheng, M., & Zhu, Y. (2014). The state of the art of wind energy conversion systems and technologies: A review. Energy Conversion and Management, 88, 332-347.

[23] Talbot, D. C., Kahraman, A., & Singh, A. (2012). An experimental investigation of the efficiency of planetary gear sets. Journal of mechanical design, 134(2), 021003.

[24] Kawalec, A., Wiktor, J., & Ceglarek, D. (2006). Comparative analysis of tooth-root strength using ISO and AGMA standards in spur and helical gears with FEM-based verification. Journal of Mechanical Design, 128(5), 1141-1158.

[25] Johnson, K. L., & Johnson, K. L. (1987). Contact mechanics. Cambridge university press.

[26] DDMotion - The Power of Control. (n.d.). Retrieved April 17, 2018, from http://www.ddmotion.com/

APPENDIX A

Matlab code: To calculate the output torque from input dimensional parameters

```
%% Single stage epicyclic gear train design
clc
clear all
close all

% Define user inputs (All dimensions are in inches)
Diametrical_Pitch='The diametrical pitch is';
Pd=input(Diametrical_Pitch);

Planet_Diameter='The planet diameter is';
Dp=input(Planet_Diameter);

Ring_Diameter='The ring diameter is';
Dr=input(Ring_Diameter);

Sun_Diameter='The sun diameter is';
Ds=input(Sun_Diameter);

% Number of teeth on the gear

Np=Dp*Pd;
Nr=Dr*Pd;
Ns=Ds*Pd;

% Configuration

% Assumption 1: The ring is driving, the planets are
driven, while the sun is stationary
w_1=Np/Nr;

% Assumption 2: The planet is stationary, sun is drive,
ring is driven
w_2=Nr/Ns;

% Assumption 3: Sun is stationary, drive planets, driven
ring
w_3=Nr/Np;

% Assumption 4: Ring Stationary, Sun drive, planet driven
w_4= Np/Ns;
```

```
M=[w_1 w_2 w_3 w_4];
w=min(M);

% Spur gear dimension calculation for pressure angle=20

Bp=0.04/Dp; %Planet backlash
Br=0.04/Dr; %Ring backlash

m=Dp/Np; % Module

C=((Dr/2)-(Dp/2)); % Center distance between the planet and
ring
Pp=((2*pi*C)/(Nr-Np)); % Circular pitch

tp=0.5*(Pp-Bp); % Planet tooth thickness
tr=0.5*(Pp-Br); % Ring tooth thickness

h=2.25*m; % Tooth depth

x_in=0.516; % Addendum modification/tooth correction for
the internal gear ie ring
x_ext=0;

Hap=(1+x_ext)*m; % Planet gear addendum
Har=(1-x_in)*m; % Ring gear addendum

Dap=(h-Hap); % Planet gear dedendum
Dar=(h-Har); % Ring gear dedendum

O=table([Dp;Np;Bp;tp;Hap;Dap],[Dr;Nr;Br;tr;Har;Dar],'Variab
leNames',{'Planet' 'Ring'},'RowNames',{'Diameter' 'No.of
teeth' 'Backlash' 'Tooth thickness' 'Addendum'
'Dedendum'});
disp(O)

% Torque and Power

% Speed values
i=50:1:500;
% Input Power and Torque
Pmax=9575; % Power corresponding to maximum wind velocity
Pmin=375; % Power corresponding to minimum wind velocity

Tmax1= (60*Pmax)./(2*pi*i);

Tmin1= (60*Pmin)./(2*pi*i);
```

```
% Output Torque

Tout_max=w*Tmax1;

Tout_min=w*Tmin1;

figure(1)
plot(i,Tout_max);
figure(2)
plot(i,Tout_min);
```

Matlab code: To calculate the dimensions from the output torque

```
%% Single stage epicyclic gear train design
%%
clc
clear all
close all

% Define user inputs (All dimensions are in inches)
Pmax=9575; % Max power corresponding to maximum wind speed
obtained from CFD chart
Pmin=375; % Min power corresponding to minimum wind speed
obtained from CFD chart

i=50:1:500;

Tmax1=(60*Pmax)./(2*pi*i);

Tmin1=(60*Pmin)./(2*pi*i);

Tout_max_output='The maximum output torque should be';
Tout_max=input(Tout_max_output);

w=Tout_max./Tmax1;%29.2590;1.1459

Tout_min=w.*Tmin1;

Np=20; %initial guess
Nr=Np./w;

Pd=20; %initial guess; Diametrical pitch
Dp=Np/Pd;
Dr=Nr/Pd;
Ds=Dr-2*Dp;

Bp=0.04/Dp; %Planet backlash
```

```
Br=0.04./Dr; %Ring backlash
m=Dp/Np; % Module

%% Gears mesh if they have the same module
Ns=Ds/m;

% Also is satisfied by the condition of Ds*Pd

%%
C=((Dr/2)-(Dp/2)); % Center distance between the planet and
ring
Pp=((2*pi*C)/(Nr-Np)); % Circular pitch

tp=0.5*(Pp-Bp); % Planet tooth thickness
tr=0.5*(Pp-Br); % Ring tooth thickness

h=2.25*m; % Tooth depth

x_in=0.516; % Addendum modification/tooth correction for
the internal gear ie ring
x_ext=0;

Hap=(1+x_ext)*m; % Planet gear addendum
Har=(1-x_in)*m; % Ring gear addendum

Dap=(h-Hap); % Planet gear dedendum
Dar=(h-Har); % Ring gear dedendum

figure(1)
plot(i,Dr)
figure(2)
plot(i,Ds)
```

APPENDIX B

Contact of elastic bodies: Hertzian distribution of pressure

In case of mating bodies, like a gear pair, a small contact area is created through elastic deformation due to the applied forces on the teeth. This created contact stresses are called Hertz contact stresses.

The Hertzian stress can be calculated using the formula

$$\sigma = \sqrt{\frac{F \times (\frac{1}{R_1} + \frac{1}{R_2})}{L \times \pi \times (\frac{(1-\upsilon_1^2)}{E_1} + \frac{(1-\upsilon_2^2)}{E_2})}}$$

Where, F is the tooth load

R_1 is the Planet radius

R_2 is the Sun radius

L is the tooth width

υ is the Poisson's ratio

E is the Youngs Modulus (E_1=E_2 since the materials are the same)

APPENDIX C

Finite Element Analysis – Contact and Mesh Report for Method 1,2,3 and 4

TABLE 1
Method 1 > Connections

Object Name	*Connections*
State	Fully Defined
Auto Detection	
Generate Automatic Connection On Refresh	Yes
Transparency	
Enabled	Yes

TABLE 2
Method 1 > Connections > Contacts

Object Name	*Contacts*
State	Fully Defined
Definition	
Connection Type	Contact
Scope	
Scoping Method	Geometry Selection
Geometry	All Bodies
Auto Detection	
Tolerance Type	Slider
Tolerance Slider	0.
Tolerance Value	4.4303e-004 m
Use Range	No
Face/Face	Yes
Face Overlap Tolerance	Off
Cylindrical Faces	Include
Face/Edge	No
Edge/Edge	No
Priority	Include All
Group By	Bodies
Search Across	Bodies
Statistics	
Connections	1
Active Connections	1

TABLE 3
Method 1 > Connections > Contacts > Contact Regions

Object Name	*Frictional - Planet Gear To Sun Gear*
State	Fully Defined

Scope	
Scoping Method	Geometry Selection
Contact	13 Faces
Target	16 Faces
Contact Bodies	Planet Gear
Target Bodies	Sun Gear
Protected	No
Definition	
Type	Frictional
Friction Coefficient	0.2
Scope Mode	Automatic
Behavior	Program Controlled
Trim Contact	Program Controlled
Trim Tolerance	4.4303e-004 m
Suppressed	No
Advanced	
Formulation	Program Controlled
Small Sliding	Off
Detection Method	Program Controlled
Penetration Tolerance	Program Controlled
Elastic Slip Tolerance	Program Controlled
Normal Stiffness	Program Controlled
Update Stiffness	Program Controlled
Stabilization Damping Factor	0.
Pinball Region	Program Controlled
Time Step Controls	None
Geometric Modification	
Interface Treatment	Add Offset, No Ramping
Offset	0. m
Contact Geometry Correction	None
Target Geometry Correction	None

TABLE 4
Method 1 > Mesh

Object Name	*Mesh*
State	Solved
Display	
Display Style	Body Color
Defaults	
Physics Preference	Mechanical
Element Order	Program Controlled
Sizing	
Size Function	Proximity and Curvature
Max Face Size	0.150 m
Mesh Defeaturing	Yes

Defeature Size	Default (7.5e-004 m)
Growth Rate	Default (1.20)
Min Size	Default (1.5e-003 m)
Max Tet Size	Default (0.30 m)
Curvature Normal Angle	Default (45.0 °)
Proximity Min Size	Default (1.5e-003 m)
Num Cells Across Gap	Default (3)
Proximity Size Function Sources	Faces and Edges
Bounding Box Diagonal	0.177210 m
Average Surface Area	4.355e-005 m²
Minimum Edge Length	3.5558e-006 m
Quality	
Check Mesh Quality	Yes, Errors
Error Limits	Standard Mechanical
Target Quality	Default (0.050000)
Smoothing	Medium
Mesh Metric	None
Inflation	
Use Automatic Inflation	None
Inflation Option	Smooth Transition
Transition Ratio	0.272
Maximum Layers	5
Growth Rate	1.2
Inflation Algorithm	Pre
View Advanced Options	No
Advanced	
Number of CPUs for Parallel Part Meshing	Program Controlled
Straight Sided Elements	No
Number of Retries	0
Rigid Body Behavior	Dimensionally Reduced
Triangle Surface Mesher	Program Controlled
Topology Checking	Yes
Pinch Tolerance	Default (1.35e-003 m)
Generate Pinch on Refresh	No
Statistics	
Nodes	913278
Elements	207420

TABLE 5
Method 1 > Mesh > Mesh Controls

Object Name	*Face Sizing*
State	Fully Defined
Scope	
Scoping Method	Geometry Selection
Geometry	38 Faces

Definition	
Suppressed	No
Type	Element Size
Element Size	1.e-004 m
Advanced	
Defeature Size	Default (5.e-005 m)
Size Function	Proximity and Curvature
Growth Rate	Default (1.2)
Curvature Normal Angle	Default (45.0 °)
Local Min Size	Default (1.e-004 m)
Proximity Min Size	Default (1.e-004 m)
Num Cells Across Gap	Default (3)
Proximity Size Function Sources	Faces and Edges

TABLE 6
Method 2 > Connections

Object Name	*Connections*
State	Fully Defined
Auto Detection	
Generate Automatic Connection On Refresh	Yes
Transparency	
Enabled	Yes

TABLE 7
Method 2 > Connections > Contacts

Object Name	*Contacts*
State	Fully Defined
Definition	
Connection Type	Contact
Scope	
Scoping Method	Geometry Selection
Geometry	All Bodies
Auto Detection	
Tolerance Type	Slider
Tolerance Slider	0.
Tolerance Value	4.2897e-004 m
Use Range	No
Face/Face	No
Face/Edge	No
Edge/Edge	No
Priority	Include All
Group By	Bodies
Search Across	Bodies
Statistics	
Connections	1

Active Connections	1

TABLE 8
Method 2 > Connections > Contacts > Contact Regions

Object Name	*Frictional - Sun Gear To Planet Gear*
State	Fully Defined
Scope	
Scoping Method	Geometry Selection
Contact	8 Faces
Target	7 Faces
Contact Bodies	Sun Gear
Target Bodies	Planet Gear
Protected	No
Definition	
Type	Frictional
Friction Coefficient	0.2
Scope Mode	Manual
Behavior	Program Controlled
Trim Contact	Program Controlled
Suppressed	No
Advanced	
Formulation	Augmented Lagrange
Small Sliding	Program Controlled
Detection Method	Program Controlled
Penetration Tolerance	Program Controlled
Elastic Slip Tolerance	Program Controlled
Normal Stiffness	Program Controlled
Update Stiffness	Program Controlled
Stabilization Damping Factor	0.
Pinball Region	Program Controlled
Time Step Controls	None
Geometric Modification	
Interface Treatment	Add Offset, No Ramping
Offset	0. m
Contact Geometry Correction	None
Target Geometry Correction	None

TABLE 9
Method 2 > Mesh

Object Name	*Mesh*
State	Solved
Display	
Display Style	Body Color
Defaults	
Physics Preference	Mechanical

Element Order	Program Controlled
Sizing	
Size Function	Curvature
Max Face Size	1.e-002 m
Mesh Defeaturing	Yes
Defeature Size	Default (5.e-005 m)
Growth Rate	Default (1.20)
Min Size	Default (1.e-004 m)
Max Tet Size	Default (2.e-002 m)
Curvature Normal Angle	Default (45.0 °)
Bounding Box Diagonal	0.171590 m
Average Surface Area	2.1715e-005 m²
Minimum Edge Length	3.5558e-006 m
Quality	
Check Mesh Quality	Yes, Errors
Error Limits	Standard Mechanical
Target Quality	Default (0.050000)
Smoothing	Medium
Mesh Metric	None
Inflation	
Use Automatic Inflation	None
Inflation Option	Smooth Transition
Transition Ratio	0.272
Maximum Layers	5
Growth Rate	1.2
Inflation Algorithm	Pre
View Advanced Options	No
Advanced	
Number of CPUs for Parallel Part Meshing	Program Controlled
Straight Sided Elements	No
Number of Retries	0
Rigid Body Behavior	Dimensionally Reduced
Triangle Surface Mesher	Program Controlled
Topology Checking	Yes
Pinch Tolerance	Default (9.e-005 m)
Generate Pinch on Refresh	No
Statistics	
Nodes	1741597
Elements	395340

TABLE 10
Method 2 > Mesh > Mesh Controls

Object Name	*Face Sizing*
State	Fully Defined
Scope	

Scoping Method	Geometry Selection
Geometry	2 Faces
Definition	
Suppressed	No
Type	Element Size
Element Size	1.e-004 m
Advanced	
Defeature Size	Default (5.e-005 m)
Size Function	Uniform
Behavior	Hard

TABLE 11
Method 2 > Mesh Edit

Object Name	*Mesh Edit*
State	Solved
Auto Detection	
Generate Automatic Mesh Connections On Refresh	No
Transparency	
Enabled	Yes

TABLE 12
Method 2 > Mesh Edit > Contact Match Group

Object Name	*Contact Match Group*
State	Meshed
Scope	
Scoping Method	Geometry Selection
Geometry	All Bodies
Definition	
Suppressed	No
Auto Detection	
Tolerance Type	Slider
Tolerance Slider	0.
Tolerance Value	4.2897e-004 m
Use Range	No
Group By	Bodies
Search Across	Bodies
Statistics	
Connections	1
Active Connections	1

TABLE 13
Method 3 > Mesh

Object Name	*Mesh*
State	Solved
Display	

Display Style	Body Color
Defaults	
Physics Preference	Mechanical
Relevance	0
Element Order	Program Controlled
Sizing	
Size Function	Adaptive
Relevance Center	Fine
Element Size	1.27e-004 m
Mesh Defeaturing	Yes
Defeature Size	Default
Transition	Slow
Initial Size Seed	Assembly
Span Angle Center	Medium
Bounding Box Diagonal	2.7518e-002 m
Average Surface Area	5.3124e-005 m²
Minimum Edge Length	2.5973e-004 m
Quality	
Check Mesh Quality	Yes, Errors
Error Limits	Standard Mechanical
Target Quality	Default (0.050000)
Smoothing	Medium
Mesh Metric	None
Inflation	
Use Automatic Inflation	None
Inflation Option	Smooth Transition
Transition Ratio	0.272
Maximum Layers	5
Growth Rate	1.2
Inflation Algorithm	Pre
View Advanced Options	No
Advanced	
Number of CPUs for Parallel Part Meshing	Program Controlled
Straight Sided Elements	No
Number of Retries	Default (4)
Rigid Body Behavior	Dimensionally Reduced
Triangle Surface Mesher	Program Controlled
Topology Checking	Yes
Pinch Tolerance	Please Define
Generate Pinch on Refresh	No
Statistics	
Nodes	13464046
Elements	3231000

TABLE 14
Method 3 > Mesh > Mesh Controls

Object Name	*Face Sizing*
State	Fully Defined
Scope	
Scoping Method	Geometry Selection
Geometry	6 Faces
Definition	
Suppressed	No
Type	Element Size
Element Size	2.54e-005 m
Advanced	
Defeature Size	Default
Behavior	Hard

TABLE 15
Method 3 > Named Selections > Named Selections

Object Name	*mesh*
State	Fully Defined
Scope	
Scoping Method	Geometry Selection
Geometry	73827 Nodes
Definition	
Send to Solver	Yes
Visible	Yes
Program Controlled Inflation	Exclude
Statistics	
Type	Manual
Total Selection	73827 Nodes
Suppressed	0
Used by Mesh Worksheet	No

TABLE 16
Method 4 > Connections

Object Name	*Connections*
State	Fully Defined
Auto Detection	
Generate Automatic Connection On Refresh	Yes
Transparency	
Enabled	Yes

TABLE 17
Method 4 > Connections > Contacts

Object Name	*Contacts*
State	Fully Defined

Definition	
Connection Type	Contact
Scope	
Scoping Method	Geometry Selection
Geometry	All Bodies
Auto Detection	
Tolerance Type	Slider
Tolerance Slider	0.
Tolerance Value	1.3997e-003 m
Use Range	No
Face/Face	Yes
Face Overlap Tolerance	Off
Cylindrical Faces	Include
Face/Edge	No
Edge/Edge	No
Priority	Include All
Group By	Bodies
Search Across	Bodies
Statistics	
Connections	47
Active Connections	26

TABLE 18
Method 4 > Connections

Object Name	*Connections*
State	Fully Defined
Auto Detection	
Generate Automatic Connection On Refresh	Yes
Transparency	
Enabled	Yes

TABLE 19
Method 4 > Connections > Contacts

Object Name	*Contacts*
State	Fully Defined
Definition	
Connection Type	Contact
Scope	
Scoping Method	Geometry Selection
Geometry	All Bodies
Auto Detection	
Tolerance Type	Slider
Tolerance Slider	0.
Tolerance Value	1.3997e-003 m
Use Range	No

Face/Face	Yes
Face Overlap Tolerance	Off
Cylindrical Faces	Include
Face/Edge	No
Edge/Edge	No
Priority	Include All
Group By	Bodies
Search Across	Bodies
Statistics	
Connections	47
Active Connections	26

TABLE 20
Method 4 > Connections > Contacts > Contact Regions

Object Name	Contact Region 23	Contact Region 24	Contact Region 25	Contact Region 26	Contact Region 27	Contact Region 28	Contact Region 29	Contact Region 30	Contact Region 31	Contact Region 32	Contact Region 33
State						Fully Defined					
Scope											
Scoping Method						Geometry Selection					
Contact	3 Faces	7 Faces	3 Faces	7 Faces	3 Faces	7 Faces	3 Faces	7 Faces	3 Faces	7 Faces	3 Faces
Target	3 Faces	7 Faces	3 Faces	7 Faces	3 Faces	7 Faces	3 Faces	7 Faces	3 Faces	7 Faces	3 Faces
Contact Bodies						Planet Gear Axle					
Target Bodies	Planet Gear Connector	Planet Gear	Planet Gear Connector	Planet Gear	Planet Gear Connector	Planet Gear	Planet Gear Connector	Planet Gear	Planet Gear Connector	Planet Gear	Planet Gear Connector
Protected						No					
Definition											
Type						Bonded					
Scope Mode						Automatic					
Behavior						Program Controlled					

Trim Contact	Program Controlled
Trim Tolerance	1.3997e-003 m
Suppressed	No
Advanced	
Formulation	Program Controlled
Small Sliding	Off
Detection Method	Program Controlled
Penetration Tolerance	Program Controlled
Elastic Slip Tolerance	Program Controlled
Normal Stiffness	Program Controlled
Update Stiffness	Program Controlled
Pinball Region	Program Controlled
Geometric Modification	
Contact Geometry Correction	None
Target Geometry Correction	None

TABLE 21
Method 4 > Connections > Contacts > Contact Regions

Object Name	Planet Gear To Sun Gear	Planet Gear To Ring Gear	Planet Gear To Sun Gear	Planet Gear To Ring Gear	Planet Gear To Sun Gear	Planet Gear To Ring Gear	Planet Gear To Sun Gear	Planet Gear To Ring Gear	Planet Gear To Sun Gear	Planet Gear To Ring Gear	Planet Gear To Sun Gear
State - Frictional						Fully Defined - Frictional					
Scope											
Scoping Method						Geometry Selection					
Contact	12 Faces	21 Faces	19 Faces	22 Faces	21 Faces	17 Faces	18 Faces	20 Faces	16 Faces	24 Faces	25 Faces
Target	10 Faces	22 Faces	16 Faces		23 Faces	22 Faces	17 Faces	20 Faces	15 Faces		23 Faces
Contact Bodies						Planet Gear					
Target Bodies	Sun Gear	Ring Gear	Sun Gear	Ring Gear	Sun Gear	Ring Gear	Sun Gear	Ring Gear	Sun Gear	Ring Gear	Sun Gear
Protected						No					
Definition											
Type						Frictional					
Friction Coefficient						0.2					
Scope Mode						Automatic					
Behavior						Program Controlled					

Trim Contact	Program Controlled
Trim Tolerance	1.3997e-003 m
Suppressed	No
Advanced	
Formulation	Augmented Lagrange
Small Sliding	Off
Detection Method	Program Controlled
Penetration Tolerance	Program Controlled
Elastic Slip Tolerance	Program Controlled
Normal Stiffness	Program Controlled
Update Stiffness	Program Controlled
Stabilization Damping Factor	0.
Pinball Region	Program Controlled
Time Step Controls	None
Geometric Modification	
Interface Treatment	Add Offset, No Ramping
Offset	0. m
Contact Geometry Correction	None
Target Geometry Correction	None

TABLE 22
Method 4 > Mesh

Object Name	*Mesh*
State	Solved
Display	
Display Style	Body Color
Defaults	
Physics Preference	Mechanical
Element Order	Program Controlled
Sizing	
Size Function	Curvature
Max Face Size	5.e-002 m
Mesh Defeaturing	Yes
Defeature Size	Default (2.5e-004 m)
Growth Rate	Default (1.850)
Min Size	Default (5.e-004 m)
Max Tet Size	Default (0.10 m)
Curvature Normal Angle	Default (45.0 °)
Bounding Box Diagonal	0.559880 m
Average Surface Area	1.6564e-004 m^2
Minimum Edge Length	4.0664e-007 m
Quality	
Check Mesh Quality	Yes, Errors
Error Limits	Standard Mechanical
Target Quality	Default (0.050000)
Smoothing	Medium
Mesh Metric	None
Inflation	
Use Automatic Inflation	None
Inflation Option	Smooth Transition
Transition Ratio	0.272
Maximum Layers	5
Growth Rate	1.2
Inflation Algorithm	Pre
View Advanced Options	No
Advanced	
Number of CPUs for Parallel Part Meshing	Program Controlled
Straight Sided Elements	No
Number of Retries	0
Rigid Body Behavior	Dimensionally Reduced
Triangle Surface Mesher	Program Controlled
Topology Checking	Yes
Pinch Tolerance	Default (4.5e-004 m)
Generate Pinch on Refresh	No

Statistics	
Nodes	2274908
Elements	893394

TABLE 23
Method 4 > Mesh > Mesh Controls

Object Name	*Hex Dominant Method*
State	Suppressed
Scope	
Scoping Method	Geometry Selection
Geometry	19 Bodies
Definition	
Suppressed	Yes
Active	No, Suppressed
Method	Hex Dominant
Element Order	Use Global Setting
Free Face Mesh Type	Quad/Tri
Control Messages	Yes, Click To Display...